International Journal of Engineering Inventions
e-ISSN: 2278-7461, p-ISSN: 2319-6491
Volume 2, Issue 5 (March 2013) PP: 01-11

Flexural Behaviour of Steel Fibers Reinforced High Strength Self Compacting Concrete Slabs

Saaid I. Zaki[1], Khaled S. Ragab[2] and Ahmed S. Eisa[3]
[1]*Associate professor, Strength of Material and Quality Control Research Institute, Housing & Building National Research Center, HBRC, Cairo, Egypt.*
[2] *Associate professor, Reinforced Concrete Research Institute, Housing & Building National Research Center, HBRC, Cairo, Egypt.*
[3] *Lecturers, Structural Engineering Department, Faculty of Engineering, Zagazig University, Zagazig, Egypt*

Abstract: *Steel Fibers Reinforced High Strength Self-Compacting Concrete (SFRHSCC) of high ductility was developed. An experimental program was carried out to evaluate the contribution of steel fibers reinforced high strength self compacting concrete for the flexural resistance of reinforced concrete slabs. A total of six reinforced concrete slabs were tested, grouped in three models. All slab models have thickness equal to 10cm, dimensions equal to 110×110cm and were reinforced by high tensile steel of 7Φ10/m. Model one is used as a control model and was cast from ordinary concrete only. Self compacting concrete with steel fibers volume fraction equal to 0.0% and 0.75% was studied in model two. High strength self compacting concrete with steel fibers volume fraction equal to 0.0, 0.75% and 1.5% was studied in model three. Taking the experimental results and performing an inverse analysis, a stress-strain diagram was obtained to characterize the post-cracking behavior of the developed SFRHSCC. In addition, a finite element analysis using* ***ANSYS***® *program, was utilized to model the tested slabs. The comparison between numerical finite element results and experimental results of the slabs previously tested by the authors is then presented and discussed. A reasonable agreement was found between the finite element analysis and the test results, therefore the finite element test program is extended further beyond the experimental limits to investigate the behavior of some more (SFRHSCC) slabs. In this extension a parametric study was carried out using the validated model to study the effects of increasing the concrete compressive strength as well as the steel fibers volume fraction.*
Keywords: *self compacting concrete; flexural resistance; steel fiber slabs; steel fiber reinforced high strength self compacting concrete (SFRHSCC); finite element analysis.*

I. Introduction

Self-compacting concrete (SCC) is characterized by high fluidity and moderate viscosity. It is able to move in the formworks and fill them uniformly under its own weight. Moreover, the use of SCC is cost- effective because this concrete does not give rise to any mechanical vibrations, it requires fewer construction workers during the casting stage, and the noise level due to mechanical vibration equipment is lower at the construction site, thereby diminishing sound effects on the environment and improving working conditions. The SCC has been widely employed to produce beams of complex shapes and/or with high density of reinforcement structures.

Besides ensuring the expulsion of air bubbles from the fresh mix with no need for mechanical vibration, the SCC must have segregation ability and bleeding strength. In concrete mixes such characteristics are obtained by addition of third generation super plasticizers and a high volume of fine materials, and/or by introduction of viscosity modifying agents Gomes [12]. From a mechanical viewpoint, both the conventional and self-compacting concretes perform less satisfactorily when they are subjected to tensile effects. This has motivated constant research into new materials that can meet the demands of structural performance. In order to achieve the best possible material; that is, a concrete with fewer constitutive deficiencies and/or a larger number of positive features, several researchers have been devoted to the optimization of the properties of concrete slabs, and new components and admixtures One way to improve the physical and mechanical properties of a concrete is the production of a composite material either via addition of steel bars commonly used as reinforcement in current civil engineering practices or by random introduction of steel fibers into the concrete mixture. A combination of both approaches is also possible, although the latter has found more restricted and less widespread use. As outlined by Kim and Mai [9], both the cement matrix and the fibers keep their original chemical and physical identities in the composite material. However, due to the presence of an interface between these two constituents, a combination of mechanical properties that cannot be obtained with the constituents alone is achieved in the hybrid concrete.

Bearing in mind the technical and economic benefits of SCC, the addition of steel fibers to this type of concrete should significantly enhance its properties in the hardened state, mainly when it is submitted to tensile stress, as in the case of concrete slabs under flexural effects. Therefore, if the use of SCC is advantageous, the

addition of steel fibers should provide it with new positive features and further possibilities of application, since a more efficient material would be obtained both at the fresh and hardened states.

This work aims to study the flexural behavior of steel fibers reinforced high strength self compacting concrete slabs (SFRHSCC), and compare the results with the flexural behavior of ordinary reinforced concrete slabs. In addition, a finite element analysis using **ANSYS**® program, was utilized to model the tested slabs. The comparison between numerical finite element results and experimental results of the slabs previously tested by the authors is then presented and discussed.

II. Experimental Work

2.1 Experimental program

Six reinforced concrete slabs were casted of rectangular shape of dimensions 110×110 cm and 10cm thickness and bottom steel was 7Φ10/m, strain gauges of 10mm length, 120ohms, and 2.04gauge factor were fixed with steel bars before casting, facing the out side of the slabs using epoxy, then a wax film was layered at the top of the strain gauge to protect it. Each slab has two strain gauges; one was placed in the mid length of the longitudinal bar and the other at the same point in the transverse bar. The following table (1) shows the standard cube compressive strength after 28 days for each slab and its description.

Table (1): Standard Cube Compressive Strength and Slab Description.

Specimen	Symbol	Description	F_{cu} 28 day (MPa)
S1	OC	Ordinary Concrete	30
S2	SCC	Self Compacted Concrete	44
S3	HSCC	High strength Self Compacted concrete	82
S4	SCC, V_f 0.75%	SCC with steel fiber 0.75%	55
S5	HSCC, V_f 0.75%	HSCC with steel fiber 0.75%	86
S6	HSCC, V_f 1.5%	HSCC with steel fiber 1.5%	90

2.2 Materials

Ordinary Portland cement was CEM1 of grade 52.5 obtained from Suez – Factory in Egypt, and complies with ESS 4756-1-2006 [15]. Silica fume was a very fine by – product powder obtained as a fume from the foundry process in the Egyptian company for Iron Foundries. Fly Ash used in the concrete mix was imported from India through Goise Company in Egypt, and complies with ASTM C618 class F [19] . The Blaine fineness of the ash is 3200 cm2/gm and its specific gravity is 2.2. Steel fibers was obtained from Master Chemical Technology Company in Egypt. Type of steel fibers is double hooked edge, 0.6mm diameter, 30mm length, 50 aspect ratio, and 850 MPa tensile strength. Fig. (1) shows the shape of steel fibers.

Coarse aggregate used in self compacted slabs was crushed dolomite with nominal maximum size of 10mm obtained from Attaka quarry , white fine aggregate was natural sand obtained from pyramids quarry in Egypt and complies with ESS 1109 , 2008 [20]. Polycorboxylate ether polymer glenium ASE 30 obtained from Basf Company in Egypt was used to produce self-compacted concrete mixes. Deformed high-grade steel bars of yield strength 400 MPa and 10 mm diameter was used as bottom steel in all slabs (7 bars/m in each direction).

2.3 Test Measurements and Instrumentation

The tested slabs were load gradually with load increment of 10 ton up to failure. The recorded data were Cracking, ultimate load capacity, concrete strains, and reinforcement strains. The vertical strains in concrete slabs were measured using linear variable displacement transducers (LVDTs). The data from (LVDTs) were connected to data acquisition system (DAS), while steel strain gauges were connected to strain indicator device to get steel strains directly.

2.4 Test results of specimens

Concrete mixes were prepared and summarized in six mixes as shown in table (2). The cement content was 350 Kg/m^3 for normal strength slabs , while increased to 500 Kg/m^3 for high strength ones. Silica fume was 15% of cement content in all mixes, fly ash was 10% of cement content in all self compacted mixes, water – binder ratio was 0.35 for all self compacted mixes, the super plasticizer ratio was 2.5% to achieve self compacted slabs with steel fibers. Steel fiber of double hooked edge was added to mix no. 4, 5 with ratio 0.75%

and to mix no. 6 with ratio 1.5%. Filling ability and viscosity of self compacted concrete were evaluated using slump flow test according to ESS 1109, 2008[17] , their results are recorded at the end of table (2).

Table (2): Concrete Mix Design

Slab No.	Type of Mix	Mix Proportions (Kg)									Fresh test	
		Cement	Sand	Coarse aggregate		Steel fibers	FA	SF	Add.	Water (Liter)	Slump (cm)	Slump flow (cm)
				C.agg1	C.agg2							
S1	OC	350	750	550	550	-	-	-	-	225	6	-
S2	SCC	350	950	950	-	-	35	52.5	10	172	26	65
S3	HSCC	500	850	850	-	-	50	75	14	180	26	66
S4	SCC V_f 0.75%	350	950	950	-	58.5	35	52.5	11	183	10	60
S5	HSCC V_f 0.75%	500	850	850	-	58.5	50	75	14	198	28	80
S6	HSCC V_f 1.5%	500	850	850	-	117	50	75	16	187	27	70

OC: Ordinary concrete, SCC: Self compacted concrete, HSCC: High strength self compacted concrete, V_f: percentage of fiber volume fraction, FA: fly ash, SF: silica fume, and Add.: admixture.

2.5 Test Procedure

All slabs were tested in flexural simply supported under load applied The set up of each test consisted of installing the tested slab in a horizontal position between machine heads, the machine heads insured that the load eccentricity was maintained at all stages of the loading and also head bearing plates were adjusted to prevent any eccentricity from wrong position. All slabs were tested using 100-ton capacity hydraulic Jacks machine in reinforced concrete laboratory in H.B.R.C. Fig. (2) shows the details of tested slabs and test setup.

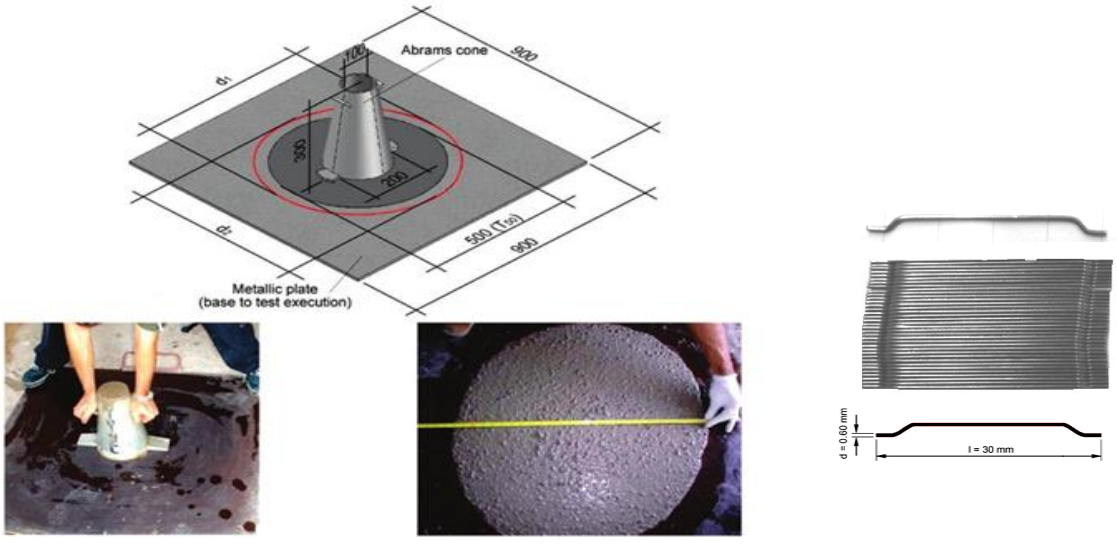

Fig. (2): Details of tested slabs and test setup

III. Test Results And Discussion

3.1 Failure modes and crack patterns of test specimens

Failure mode of all tested specimens was flexural failure (FF), Failure by flexure occurred by yielding of the steel reinforcement, followed by crushing of the concrete in the compression zone at very large deformations. Table (3) shows the test results of all tested specimens including; specimens' description, ultimate loads, and failure modes.

All tested specimens were designed to fail in flexure with tensile mode, which was characterized by the formation of cracks in the tensile stress zone (bottom and side faces), then yielding of steel bars. Generally, as the load was increased, cracks started to appear and extended from that perimeter under the loading line due to the bending moment toward the supported edges of the tested slabs. At the same time, the cracks increased in number and became wider at the center region parallel to the line of applied loads for all the tested slabs. A complete failure occurred by increasing the load. The slabs with steel fibers failed in more ductile mode. In these slabs, typical cracking patterns on the bottom surface of these slabs were observed, cracks formed uniformly with smaller width due bridging effect of steel fibers. By observing the test results, it can be concluded that the steel fibers improve significantly concrete ductility. Fig. (3) shows the failure modes and crack patterns of the tested specimens.

Table (3): Test results

Specimen	Concrete properties	Compressive strength, F_{cu} (MPa)	Fiber volume fraction, V_f (%)	Ultimate load, V_u (KN)	Failure mode
S1	Ordinary Concrete	30	0.0	113	FF
S2	SCC	48	0.0	120.5	FF
S3	HSCC	84	0.0	122	FF
S4	SCC	54	0.75	151	FF
S5	HSCC	87	0.75	126.5	FF
S6	HSCC	90	1.5	145	FF

(a) Slab S1; ordinary concrete without steel

(b) Slab S2; SCC without steel fibers

(c) Slab S3; HSCC without steel fibers

(d) Slab S4; SCC with steel fibers (0.75%)

(e) Slab S5; HSCC with steel fibers (0.75%)

(f) Slab S6; HSCC with steel fibers (1.5%)

(g) Slab S4; HSCC with steel fibers (0.75%)

(h) Slab S6; HSCC with steel fibers (1.5%)

Fig. (3): Failure modes and crack patterns of the tested specimens – bottom and side surfaces

3.2 Flexural behavior of test specimens

Based on the experimental results, the behavior of the tested slabs is discussed in terms of observed behavior, concrete type, ultimate load, load-deflection curves, and failure mode as shown in table (3) and figures from (4) to (7) which indicate that the relationship between applied load and deflection at the center of the slab was typical for all the tested slabs, an approximate linear increase behavior followed by a nonlinear behavior until failure.

Using self compacting concrete (SCC) causes significant difference in the behavior of the tested slabs and improves the flexural resistance as shown in fig. (4). Steel fibers increase considerably flexural strength of self compacting concrete slabs and this increase is because of steel fibers help to bridge cracks in the whole concrete volume and transfer tensile stress through two opposite faces of cracks until the fibers are totally pulled-out or broken. For this reason, in stage of initiation and propagation of cracks, tensile zone of steel fibers self compacting concrete slabs (SFRSCC) still sustains load. This increases concrete tensile strength and indirectly leads to increase the flexural strength of slabs. Fig. (5) shows clearly effect of steel fibers on the flexural strength of self compacting concrete slabs, for steel fibers self compacting concrete slabs (SFRSCC) the flexural strengths increased by 25.3% at fiber volume fraction of (0.75%) in comparison with that of steel fibers self compacting concrete slabs (SFRSCC) without steel fibers as given in table (3).

All steel fibers self compacting concrete slabs (SFRSCC) showed a gradual and ductile behavior beyond the maximum load in comparison with reinforced concrete slabs without fiber content. It can be noticed from test results that, the flexural strength in terms of ultimate load increased significantly with a corresponding increase in the concrete compressive strength.

For steel fibers high strength self compacting concrete slabs (SFRHSCC), the flexural strengths increased by 18.8% at fiber volume fraction of (1.5%) in comparison with that of high strength self compacting concrete slabs (HSCC) without steel fibers as given in table (3). In contrast, flexural strengths increased slightly by 3.7% at fiber volume fraction of (0.75%) in comparison with that of high strength self compacting concrete slabs (HSCC) without steel fibers as given in table (3). The flexural behaviors of (SFRHSCC) slabs were almost identical close to the maximum load as shown in fig. (6), though the fiber volume fraction was varied. The maximum loads did not linearly increase with increasing the fiber volume fraction. They showed that the increase of the flexural strength of (SFRHSCC) slabs became sensible from the fiber volume fraction over 0.75% to 1.5%.

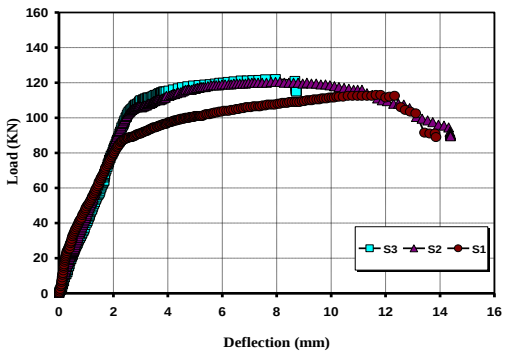

Fig. (4): Slabs of different concrete types without steel fibers

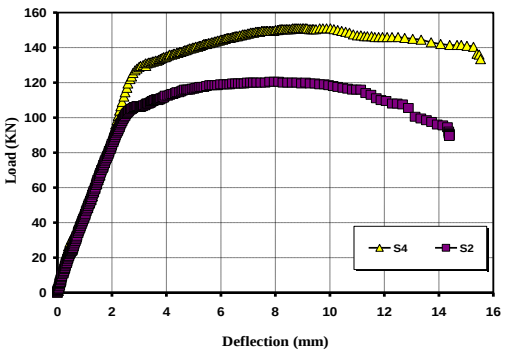

Fig. (5): Effect of steel fibers on SCC

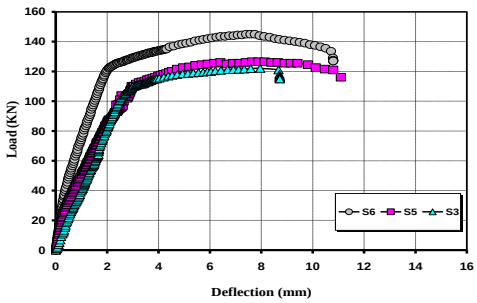

Fig. (6): Effect of steel fibers on HSCC

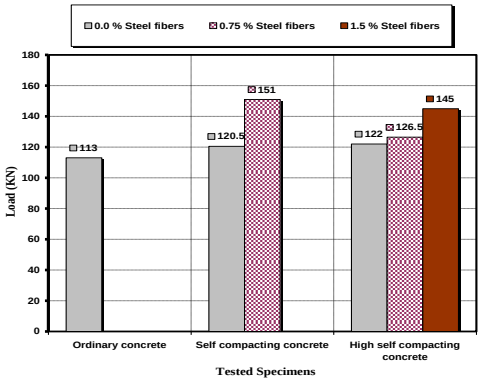

Fig. (7): Flexural strengths for all the tested specimens

IV. Finite Element Analysis

4.1 Modeling

4.1.1 Concrete elements

SOLID 65 element was used to model the concrete. **SOLID 65** element is an eight node soild element and has 3 displacement and 3 rotation degrees of freedom at each node. In other words, six degree of freedom at each node . The element took the shape of a rectangular prism. The most important aspect of the **SOLID 65** element is the treatment of nonlinear material properties. The response of concrete under loading is characterized by a distinctly nonlinear behavior. The typical behavior expressed in the stress-strain relationship for concrete subjected to uniaxial loading is shown in fig. (8). **SOLID 65** element considers smeared crack in tension and crushing in compression, and its failure criterion is given by:

$$F/f_c - S\ P\ 0 \qquad (1)$$

Where *F* is a function of the principal stresses, *S* is the Willam and Warnke [105] failure surface, and f_c is the material compressive strength. When eq.1 is satisfied, the material will crack if any principal stress is tensile and will crush when all principal stresses are compressive. The Willam and Warnke [2] failure surface used in **ANSYS**® is defined by five parameters, which are the concrete uniaxial compressive strength (f_c), concrete tensile strength (f_t), concrete biaxial compressive strength (f_{cb}), concrete biaxial compressive strength superimposed on a hydrostatic stress state (f_1), concrete uniaxial compressive strength superimposed on a hydrostatic stress state (f_2).

The material model from **ANSYS**® considers perfect bond between reinforcement and concrete. Moreover, **ANSYS**® allows the definition of two shear transfer coefficients, one for opened cracks and the other for closed cracks that are used to model cracks. Concrete cracking is represented by modifying the stress-strain relationship trough the introduction of a failure plane normal to the crack surface. The shear transfer coefficient represents a reduction on the material shear strength that introduces slip trough the crack surface. Apart from cracking and crushing, ***SOLID 65*** can also represent plasticity and creep, and allows the introduction of a reinforcement material in up to three directions. The reinforcement that has uniaxial stiffness and is considered smeared on the concrete finite element, can also present plasticity and creep. The elastic modulus of concrete was calculated by using the slope of the tangent to the stress–strain curve through the zero stress and strain point for each model. The Poisson ratio is taken as 0.2. The ultimate uni-axial compressive and tensile strengths of concrete were taken from the laboratory test results.

The crack interface shear transfer coefficient β_t for open cracks was assumed to range from 0.1 to 0.5 while for closed cracks the shear transfer coefficient β_c was assumed to range from 0.7 to 0.9. The higher ranges of values were assumed for **SFRC** as it was expected that the fibers would contribute significantly to shear transfer across a crack.

4.1.2 Steel fibers elements

The effectiveness of steel fibers in increasing the flexural and tensile strength of the concrete, at least partially, depends on the number of fibers per unit cross-sectional area of concrete. The fraction of the entire volume of the fiber was modeled explicitly as it was expected to contribute to the mobilization of forces required to sustain the applied loads after concrete cracking and provide resistance to crack propagation. The number of fiber per unit area was calculated in this study, based on the probability approach given by Parviz and Lee [5]. The equations given by [5,3] to predict the number of fibers per unit crosssectional area of concrete are of the form:

$$N_f = \alpha^1 \upsilon_f / N_f \qquad (2)$$

where α^1 is the orientation factor which ranges from 0.41 to 0.82 [110].

Orientation of these fibers in concrete and consequently the number of fibers per unit cross-sectional area is influenced not only by the boundaries restricting the random orientation of fibers, but also by the fact that the fibers tend to settle down and reorient in horizontal planes when the fiber concrete matrix is vibrated during casting. As a result of vibration, the random orientation of fibers in concrete moves away from a three-dimensional condition to a two-dimensional condition. Hence, the value α^1 was taken based on the ***2D*** orientation of the fibers as equal to 0.645 (average value of 0.55–0.74 proposed by Parviz and Lee [5]). Thus the number of fibers per finite element is given by:

$$A_f = \alpha^1 \upsilon_f A_e \qquad (3)$$

Where A_e is the cross-sectional area of a concrete element. Thus knowing α^1, the number of fiber between each element was calculated for each finite element mesh. The elements lying at the boundary carry half of the area of fibers used in interior of the **FE** mesh. The equivalent fiber reinforcement is considered

smeared in the finite element in three orthogonal directions that coincide with the cartesian directions. The equivalent fiber reinforcement has as parameters; Young's modulus E_s = 2000000 MPa, Poisson ratio ν=0.3, and equivalent tensile strength f_s = 1500 MPa.

4.1.3 Reinforcement steel elements

Modeling of reinforcing steel in finite elements is much simpler than the modeling of concrete. ***LINK 8*** element was used to model steel reinforcement. This element is a ***3D*** spar element and it has two nodes with three degrees of freedom – translations in the nodal x, y, and z directions. This element is also capable of plastic deformation. A perfect bond between the concrete and steel reinforcement is considered. However, in the present study the steel reinforcing was connected between nodes of each adjacent concrete solid element, so the two materials shared the same nodes. Steel reinforcement in the experimental work was constructed with typical steel reinforcing bars. Elastic modulus and yield stress for the steel reinforcement used in **FE** study follow the material properties used for the experimental work. The steel for the **FE** models is assumed to be an elastic-perfectly plastic material as shown in fig. (9). A Poisson's ratio of 0.3 is used for the steel reinforcement.

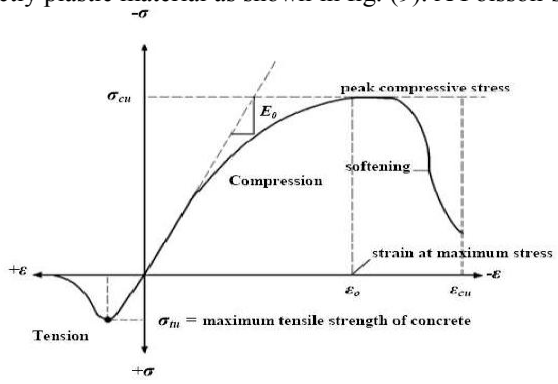

Fig.(8): Typical Uniaxial Compressive and tensile Stress-Strain Curve for Concrete [4].

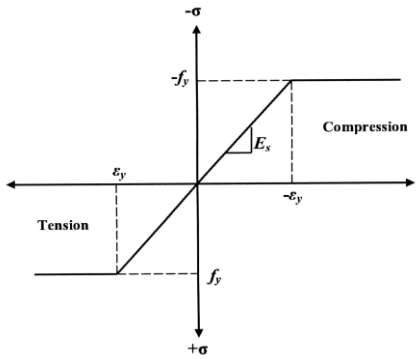

Fig.(9): Idealized stress-strain curve for steel

4.2 Nonlinear analysis in *ANSYS*®

The status transition of concrete from an uncracked to cracked state and the nonlinear material properties of concrete in compression and steel as it yields cause the nonlinear behavior of the structures under loading. In nonlinear analysis, the total load applied to a finite element model is divided into a series of load increments called load steps. At the completion of each incremental solution, the stiffness matrix of the model is adjusted to reflect nonlinear changes in structural stiffness before proceeding to the next load increment. The Newton–Raphson equilibrium iterations for updating the model stiffness were used in the nonlinear solutions. Prior to each solution, the Newton–Raphson approach assesses the out-of-balance load vector, which is the difference between the restoring forces (the loads corresponding to the element stresses) and the applied loads. Subsequently, the program carries out a linear solution using the out-of-balance loads and checks for convergence. If convergence criteria are not satisfied, the out-of-balance load vector is re-evaluated, the stiffness matrix is updated, and a new solution is carried out. This iterative procedure continues until the results converge.

In this study, convergence criteria for the reinforced concrete solid elements were based on force and displacement, and the convergence tolerance limits were initially selected by analysis program. It was found that the convergence of solutions for the models was difficult to achieve due to the nonlinear behavior of reinforced concrete. Therefore, the convergence tolerance limits were increased to a maximum of five times the default tolerance limits (0.5% for force checking and 5% for displacement checking) in order to obtain the convergence of the solutions. In order to verify the test results of the experimental data, the finite element was performed to test same models pre-tested experimentally. **ANSYS**® elements, material properties, and assumptions are used in the models analysis. To obtain satisfactory results from the ***SOLID 65*** element, a rectangular mesh is recommended. Therefore, the mesh was setup such that square or rectangular elements were created as shown in fig. (10). Bar reinforcement, boundary conditions, and applied loads are shown in fig. (10) as well.

4.3 Finite element results

By using the **ANSYS**® postprocessing package, it can follow the stress distribution across the tested slabs of the finite element model at each load increment. In addition, from data files, the load at each increment can be obtained. Therefore failure capacity and deflection levels can be determined. The final loads for the finite

element models are the last applied load step before the solution diverges due to numerous cracks and large deflections.

A comparison between experimental and finite element results is summarized in table (4) in terms of ultimate load and maximum vertical deflection. It is clear from the results listed in table (4) that the finite element analysis underestimates the ultimate loads of tested slabs by ratios ranged from 0.91 to 0.98 compared to experimental values. Also underestimate the maximum deflection by ratios ranged from 0.80 to 0.96 compared to experimental values.

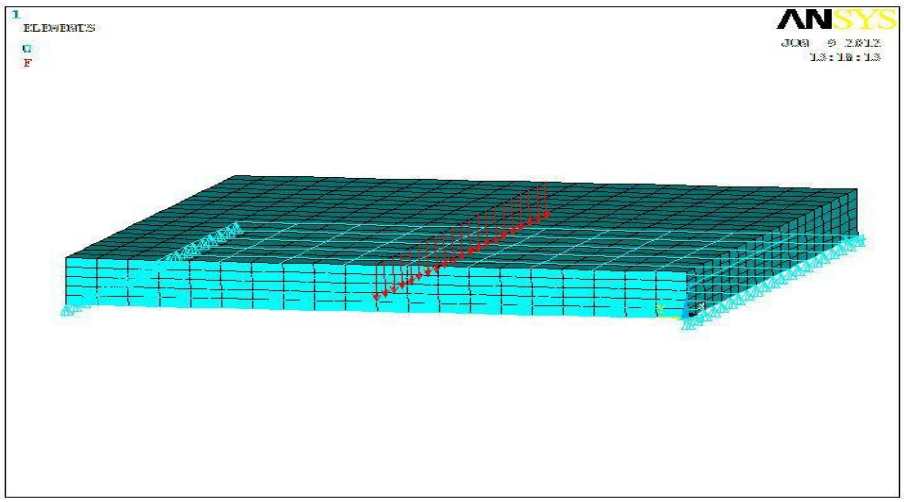

Fig. (10): Finite element mesh for a typical slab model

Table (4): Comparison between experimental and finite element results

Model	Finite Element Ultimate Load P_{uf} (KN)	Finite Element Ultimate Load P_{ue} (KN)	P_{uf} / P_{ue}
S1	103	113	0.91
S2	107	120.5	0.89
S3	108	122	0.89
S4	137	151	0.91
S5	110	126.5	0.87
S6	126	145	0.87

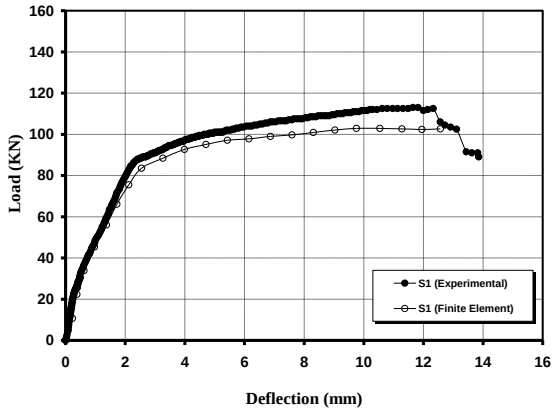

Fig. (11): Comparison of load-deflection curves, S1

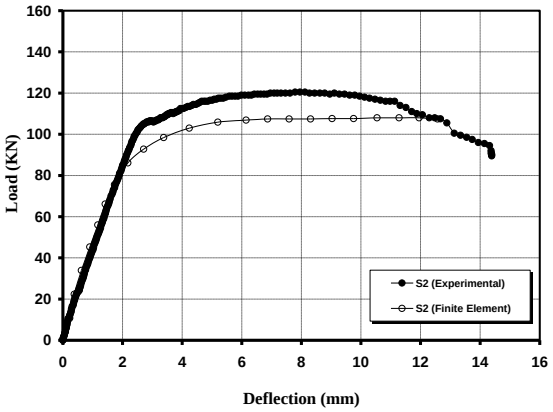

Fig. (12): Comparison of load-deflection curves, S2

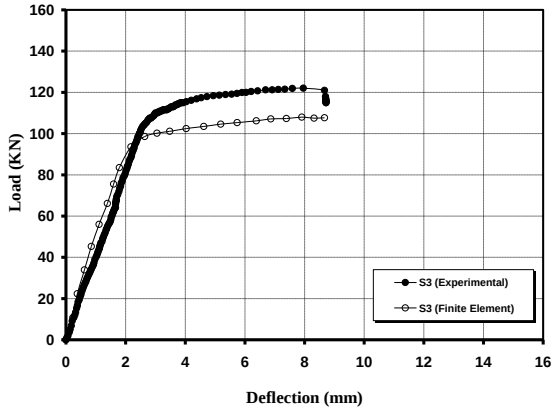

Fig. (13): Comparison of load-deflection curves, S3

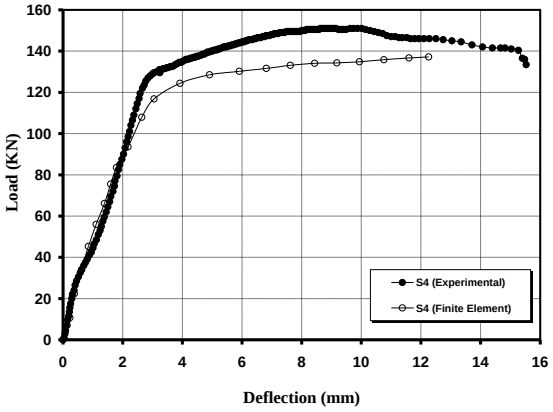

Fig. (14): Comparison of load-deflection curves, S4

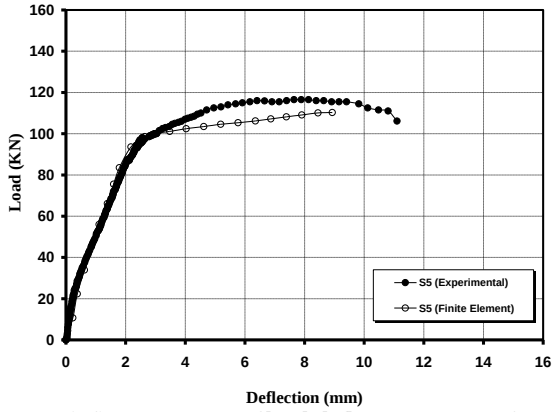

Fig. (15): Comparison of load-deflection curves, S5

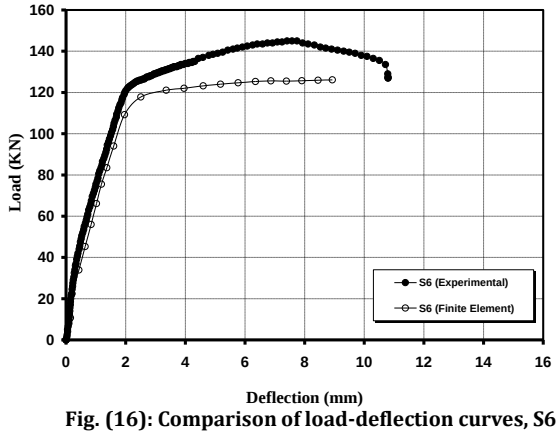

Fig. (16): Comparison of load-deflection curves, S6

Figures from (11) to (16) showed the finite element load- deflection curves in comparison with the experimental ones, the comparison showed that the ratio of ultimate loads predicted by finite element to experimental values ranged from 0.87 to 0.91. The curves showed good agreement in finite element analysis with the experimental results throughout the entire range of behavior and failure mode, for all slabs, the finite element models are stiffer than the actual slabs in the linear range. Several factors may cause the higher stiffness in the finite element models. The bond between the concrete and steel reinforcement is assumed to be perfect (no slip) in the finite element analyses, but for the actual slabs the assumption would not be true slip occurs, therefore the composite action between the concrete and steel reinforcement is lost in the actual slabs. Also the microcracks produced by drying shrinkage and hardling are present in the concrete to some degree. These would reduce the stiffness of the actual slabs, while the finite element models do not include microcracks due to factors

that are not incorporated into the models. After the initiation of flexural cracks, the slab stiffness was reduced and the linear load –deflection behavior ended when the internal steel reinforcement began to yield.

4.4 Parametric Study

The closeness of the experimental and the finite element results indicate that **ANSYS**® can be used to model the behavior of steel fibers reinforced high strength self-compacting concrete (SFRHSCC) slabs in flexure and predict the maximum load carrying capacity as well. Therefore the finite element test program is extended further beyond the experimental limits to investigate the behavior of some more SFRHSCC slabs. In this extension a study of different parameters were considered. A parametric study will be carried out using the validated models to study the effects of changing the steel fibers volume fraction as well as the concrete compressive strength.

Table (5) and figures (17, 18) show the values of ultimate loads according to the variation of volume fraction of steel fibers from 0% to 4.5%, and the variation of concrete compressive strengths (F_{cu} = 80, 100, 120, 140 MPa).

Table (5): Numerical results of the parametric study

Compressive strength, F_{cu} (MPa)	Slab model	Fiber volume fraction, V_f (%)	Ultimate Load, P_{ue} (KN)
80	1	0.00	106
	2	0.75	107
	3	1.50	109
	4	2.25	118
	5	3.00	121
	6	3.75	124
	7	4.50	129
100	8	0.00	122
	9	0.75	124
	10	1.50	126
	11	2.25	128
	12	3.00	131
	13	3.75	138

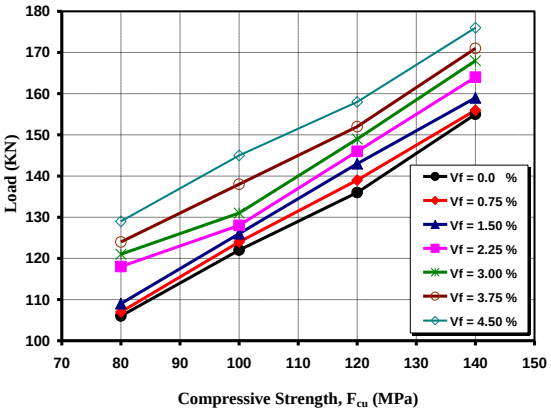

Fig. (17): Effect of (F_{cu}) on flexural strength

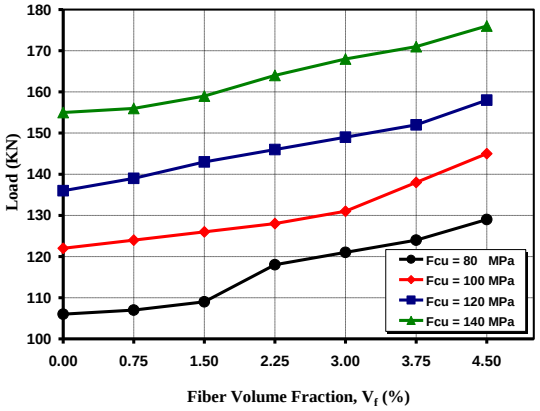

Fig. (18): Effect of (V_f%) on flexural strength

According to the results of the parametric study listed in table (5) and plotted in figures (17, 18) to study the effects of changing the steel fibers volume fraction as well as the concrete compressive strength on the behavior of SFRHSCC slabs in flexure, the following observations were obtained:

- Increasing the steel fibers volume fraction from 0.75% to 4.5% for SFRHSCC slabs increases the flexural strengths by average value ranges from 1% to 22%.

- The increase in flexural strengths for SFRHSCC slabs decreases by increasing the concrete compressive strength, at steel fibers volume fraction (4.5%) the increase in flexural strengths are (22%, 18.9%, 16.2%, 13.5%) at concrete compressive strengths (80, 100, 120, 140MPa) respectively.

V. Conclusions

Based on the results obtained from study, the following conclusions can be drawn:

1. Using self compacting concrete (SCC) causes significant difference in the behavior of the tested slabs and improves the flexural resistance.

2. All steel fibers self compacting concrete slabs (SFRSCC) showed a gradual and ductile behavior beyond the maximum load in comparison with reinforced concrete slabs without fiber content because inhibit the initiation and growth of cracks.

3. The study showed that the increase of the flexural resistance of (SFRHSCC) slabs became insensible compared with (SFRSCC).

4. The flexural strengths increased by 25.3% at fiber volume fraction of (0.75%) in comparison with that of steel fibers self compacting concrete slabs (SFRSCC) without steel fibers

5. Increasing the steel fibers volume fraction from 0.75% to 4.5% for SFRHSCC slabs increases the flexural strengths by average value ranges from 1% to 22% at concrete compressive strengths 80 MPa and decreases this rang by increasing the concrete compressive strength.

6. Steel fibers improve the flexural strength resistance of the slabs considerably. Using steel fibers with volume fraction equal to 0.75% with self compacted concrete is the ideal percentage to increase the flexural strength resistance slabs.

7. The finite element analysis underestimates the ultimate loads of tested slabs by ratios ranged from 0.91 to 0.98 compared to experimental values. Also underestimate the maximum deflection by ratios ranged from 0.80 to 0.96 compared to experimental values.

8. The closeness of the experimental and the finite element results indicate that **ANSYS**® can be used to model the behavior of steel fibers reinforced high strength self-compacting concrete (SFRHSCC) slabs in flexure and predict the maximum load carrying capacity as well.

References

[1] James PR, James AM. , " Tensile strength of concrete affected by uniformly distributed and closely spaced short lengths of wire reinforcement, " ACI J 1964;61(6):657–70.

[2] Willam K.J. and Warnke E.P., "Constitutive model for triaxial behaviour of concrete, " Structural Engineering International, 1975; 19; 1-30.

[3] Naaman AE, Moaven ZF, McGarry FJ. , " Probabilistic analysis of fiber reinforced concrete, " Proc ASCE 1974;100(EM2):397–413.

[4] Bangash, M. Y. H. (1989), Concrete and Concrete Structures: Numerical Modeling and Applications, Elsevier Science Publishers Ltd., London, England.

[5] Parviz S, Cha-Don L. , " Distribution and orientation of fibers in steel fiber reinforced concrete, " ACI Mater J 1990;87(5):433–9.

[6] Japan Society of Civil Engineers (1997). "Recommendation for Design and Construction of Concrete Structures Using Continuous Fiber Reinforcing Materials ", Concrete Engineering Series 23, ed. by A. Machida, JSCE, Tokyo, Japan .

[7] Mindess, S., Adebar, P., and Henley, J., "Testing of Fiber- Reinforced Structural Concrete Elements," Proceedings of ACI International Conference on High-Performance Concrete: Design and Materials and Recent Advances in Concrete Technology, ACI SP-172, 1997, pp. 495~515.

[8] ANSYS (1998), ANSYS User's Manual Revision 5.5, ANSYS, Inc., Canonsburg, Pennsylvania.

[9] KIM, J-K.; MAI, Y-W. (1998) Engineered interfaces in fiber reinforced composites. Elsevier Science Ltd. 1_{st} Ed. Oxford, U.K, 1998. ISBN 0-08-042695-6.

[10] McHarg PJ, Cook WD, Mitchell D, and Young-Soo Y (2000). Benefits of concentrated slab reinforcement and steel fibers on performance of slab-column connections. ACI Structural Journal. 97(2), pp. 225-234 .

[11] ACI 318M-02. Building code requirements for structural concrete. American Concrete Institute, Farmington Hills, Michigan, 2002.

[12] Gomes, P. C. C. Optimization and characterization of high-strength self-compacting concrete, Barcelona, 2002, Tese (doutorado) - Curso de Pós-Graduação em Engenharia Civil, Universitat Politècnica de Catalunya, 150 p.

[13] ACI 440, (2003). "Guide for the Design and Construction of Concrete Reinforced with FRP Bars," ACI 440.1R-03, American Concrete Institute, Farmington Hills, MI .

[14] Okamura H. and Ouchi M., "Self Compacting Concrete", Journal of Advanced Concrete Technology, Vol. 1, Japan, April, 2003.

[15] Egyptian Standard specification for ordinary Portland cement (ESS 4756.-1-2006) , Produced from General Organization for specification and Quality in Egypt. (1)

[16] Egyptian Technical Specifications for self-compacted concrete, Ministerial Descion No. 360-2007

[17] Egyptian Standard specifications for aggregates, ESS 1109, 2008. (3)

[18] Produced from Housing and Building National Research Center Egypt.(4)

[19] American Standard specifications for Fly Ash, ASTM C618 class F.(2)

[20] ACI Committee 318, "Building Code Requirements for Structural Concrete", (ACI 318-08) and Commentary (ACI 318R-08), American Concrete Institute, Farmington Hills, MI, 2008, pp.465.